Transformation Cosmology

Huanyang Chen[1]*, Sicen Tao[1], Jakub Bělín[2], Johannes Courtial[2+] and Rong-Xin Miao[3]
[1] Institute of Electromagnetics and Acoustics and Key Laboratory of Electromagnetic Wave Science and Detection Technology, Xiamen University, Xiamen 361005, China
[2] School of Physics & Astronomy, College of Science & Engineering, University of Glasgow, Glasgow G128QQ, UK
[3] School of Physics and Astronomy, Sun Yat-Sen University, 2 Daxue Road, Zhuhai 519082, China
* kenyon@xmu.edu.cn
+ Johannes.Courtial@glasgow.ac.uk

Abstract: Recent observation of black hole and gravitational wave has stirred up great interest of Einstein's general relativity. In optical system, the "optical black hole" has also been a key topic in mimicking black holes. Another good way to study or mimic general relativity effects is based on transformation optics. In this paper, we propose a way by utilizing transformation optics theory to directly obtain the equivalent isotropic refractive index profiles which are the analogies of some static spaces of general relativity, such as de Sitter space, Anti de Sitter space, and Schwarzschild black hole. We find that, the analogue of de Sitter space is the Poincaré disk, while Anti de Sitter space is equivalent to Maxwell's fish eye lens. In particular, we prove that the "optical black hole" actually has infinite number of photon spheres, while our black hole only has a single one, which is closer to the real black hole. We study the effect from both geometric optics and wave optics. It can also be generalized to mimic any kind of metrics. Furthermore, with the isotropic refractivity index profile, we visualize the gravitational lensing effect of black hole from our software TIM. The image not only recovers the donut-liked halo of black hole, but also shows other phenomena.

I. Introduction

Einstein's general relativity [1] is actively recalled recently as it well predicted gravitational wave [2] and black hole [3] that lately observed. Besides, it would be fantastic if the celestial mechanics could be mimicked in laboratories. A novel method is called general relativity in electrical engineering [4], which could be used to mimic similar cosmic phenomena by complicated electromagnetic material parameters, like that from transformation optics [5, 6, 7]. Transformation optics, thanks to its convenience and flexibility on manipulating electromagnetic waves, has a great many applications, including, but not limited to invisibility cloaks[5, 6], rotators [8, 9], concentrators[10, 11], perfect lenses[12, 13] and electromagnetic cavities[14]. In addition, as mentioned before, optical analogues of general relativity effects which demonstrated by four-dimensional (4D) metrics have been designed. For example, a simulation of a derived permittivity tensor profile and a permeability has been proved to be equivalent to a Schwarzschild black hole [15]. A generalized analytical formalism for developing analogues of spherically symmetric static black holes was discussed [16]. The equivalent time-dependent material parameters can be used to achieve the cosmological redshift [17]. Other works, such as to mimic de Sitter space [18, 19], time travel effect [20] have also been proposed based on this electrical general relativity [4].

However, this method requires complicated material parameters, thereby making experiments difficult to implement. Although uniaxial medium for Schwarzschild-(anti-)de Sitter spacetime could be obtained by constructing the Tamm medium which constitutes simple homogenized component parameters, there still exists many restrictions and tedious process [21]. Nevertheless, by performing transformation optics [22], the complicated parameters could be simplified into isotropic refractive index profiles [23], which not only make calculation simpler [24], but also make experiment more feasible, such as the black holes in microwave [25] and visible frequencies [26]. Other general relativity effects, such as Einstein's ring [27] and cosmic string [28], have also been mimicked for visible frequencies.

On the other hand, the topic of mimicking black hole has been studied for a long time. The "optical black hole" [23] has a good absorption efficiency. FDTD calculation method has been used to prove the absorption property [24]. The corresponding experiment results [25] also show great agreement with the theoretical work [23]. However, we will prove that this "optical black hole" actually contains infinite number of photon spheres. It is exactly rather a light absorber than a black hole. While our black hole model which carries only one photon sphere shows more similarity with the realistic black hole.

In this paper, we come up with some spatial mappings, combining the metric formulas, to get the isotropic material parameters. We will show the analogue spaces (de Sitter space and black hole) both in geometric optics and in wave optics. We will prove that the equivalent spaces of de Sitter space and Anti de Sitter space are exactly the Poincaré disk and Maxwell's fish eye lens, respectively. Moreover, visualization of black hole will be demonstrated. It reveals the details outside the event horizon and gives us a more intuitional image of gravitational lensing effect around the event horizon. Our black hole model has only one photon sphere, so that we could see the donut-liked halo of black hole. It should be noted that our model contains only spatial transformation without considering the time dimension. That is, we just concern about the space change of three-dimensional (3D) optical metric. Therefore, we don't need to worry about the causal structure's swapping in 4D manifold of space-time [29][30]. Furthermore, we believe that, compared with anisotropic material parameters, the isotropic refractive index profiles can be easier to fabricate. For instance, the geodesic lenses give us some hints on investigating light propagation on curved surfaces that can be connected to this kind of refractive index profiles [31] [32].

II. Calculation and Results

We start from a general metric form of

$$ds^2 = -f(r)dt^2 + \frac{1}{f(r)}dr^2 + r^2 d\Omega^2 . \quad (1)$$

In this letter, we will show that such a metric form could be equivalent to a refractive index profile by transformation optics. With this method, experimental realization becomes much easier and simulations of ray-optical phenomena can be performed in custom ray-tracers, e.g. Dr. TIM [33].

We perform a mapping in the radial direction $r = r(R)$ (or $R = R(r)$), the metric is then

transformed into the following form,

$$ds^2 = -f(r(R))dt^2 + \frac{dr^2/dR^2}{f(r(R))}dR^2 + \frac{r^2}{R^2}R^2 d\Omega^2 . \quad (2)$$

To obtain a spacial isotropic metric, we should let[22]

$$\frac{dr^2/dR^2}{f(r(R))} = \frac{r^2}{R^2} . \quad (3)$$

which could be used to obtain the required mapping by considering suitable boundary condition. After that, it would be easy to get the equivalent refractive index profile [22],

$$n(R) = \left(g/g_{00}\right)^{\frac{1}{2}} = \frac{|dr(R)/dR|}{f(r(R))} = \frac{r(R)}{R\sqrt{f(r(R))}} . \quad (4)$$

The inverse process is also very interesting. Given the refractive-index profile, one can solve Eq. (4) for $f(r)$ to get a corresponding space-time metric, whose form is given by Eq. (1), although such a metric is not exactly a solution of Einstein's field equations.

For example, when $f(r) = 1 - \frac{r^2}{a^2}$ ($r \le a$, the horizon), the metric is for de Sitter space. After the mapping of $r = \frac{2R}{1 + \frac{R^2}{a^2}}$, according to Eq. (4), the equivalent refractive index profile should be,

$$n(R) = \frac{2}{1 - \frac{R^2}{a^2}} \quad \text{(for } R \le a \text{ , the transformed horizon).} \quad (5)$$

Using the commercial software COMSOL Multiphysics as the simulation tool, figure 1(a) shows light rays emerging from a point source, situated at an arbitrary point inside the space. All the emitted rays become perpendicular to the horizon $R = a$. Actually, Eq. (5) is exactly the Poincaré disk metric. The geometry of the Poincaré disk is limited in a unit disk, in which straight lines consist of all circular arcs that are orthogonal to the boundary of the disk [34][35]. It means that light will never reach the boundary and anyone wherever he or she is in such a space will always be the center of the universe. This is an inverse effect of a black hole, which will be further analyzed in the later section. We also plot the field pattern in wave optics in Fig. 1(b). For simplicity, we performed the above simulations in two-dimensional cylindrical coordinate system, because it has the same optical behaviors as that in three dimensions and is easier to simulate or realize in table-top devices. It should be noted that in wave optics perspective we set the boundary radius a little bit smaller than a (here is 1) to avoid reaching the singularity of the horizon and to better perform the field pattern. A perfectly matched layer was added to truncate the space. This profile will change the cylindrical wave front from any point into a cylindrical wave front with its center at the origin when approaching the horizon, which is also similar to the zero index lens [36].

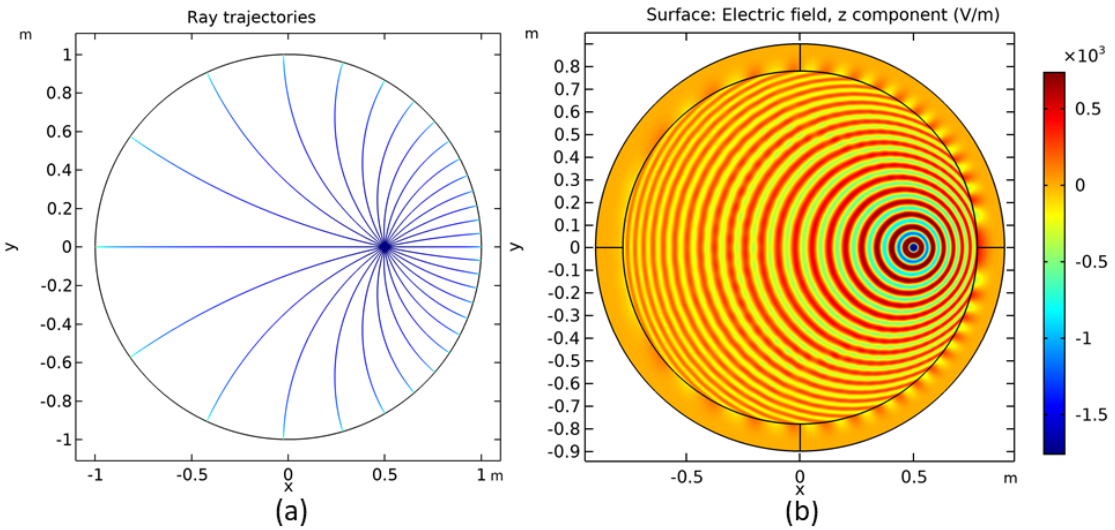

Fig. 1 A point source inside the de Sitter profile (Eq. 5) (a) the ray trajectories; (b) the field pattern.

When $f(r)=1+\frac{r^2}{a^2}$, the metric is for Anti de Sitter space. After the mapping of $r=\frac{2R}{1-\frac{R^2}{a^2}}$, the equivalent refractive index profile should be,

$$n(R)=\frac{2}{1+\frac{R^2}{a^2}} \quad (6)$$

which is the famous Maxwell's fisheye lens [37], a perfect lens with positive refraction. Similar process could be performed for any $f(r)$, which are very promising to study various metrics in laboratories. In the letter, we hope to recall the black hole in [15], where $f(r)=1-\frac{L}{r}$ ($r\geq L$, the horizon). A similar trick suggests the mapping of $r=\frac{(R+\frac{L}{4})^2}{R}$, which was also called as an isotropic radial coordinate transformation [38], and the equivalent refractive index profile should be,

$$n(R)=\frac{(R+\frac{L}{4})^3}{R^2(R-\frac{L}{4})} \quad \text{(for } R\geq\frac{L}{4}\text{, the transformed horizon).(7)}$$

Here, similar to the previous work [15, 23], we take the following parameters for the inner core. The imaginary part works as a loss term to absorb the fields at the event horizon.

$$n(R)=\frac{(R+\frac{L}{4})^3}{R^2(R-\frac{L}{4})}(1+i) \quad \text{(for } R<\frac{L}{4}\text{, the transformed horizon).(8)}$$

It reminds us of the interior of black hole [39, 40], which is exact solution of Einstein's field equation. It could help us better understand the black hole with a view point of an observer inside the event horizon, and make the research more complete. In this paper, we will pay more attention on the studies outside the black hole and not go into details of the inner core, we use the above equation (8) as an absorber for our black hole. Nevertheless, the interior of black hole is still an interesting topic for the future research, as the interior structure of realistic black holes have not been satisfactorily determined, and are still open to considerable debate, as stated in reference [39].

We will prove that the profile of Eq. (7) indeed mimics a Schwarzschild black hole. Before we get into the details, let us recall the isotropic black hole that is usually used in metamaterials [23]. The profile is

$$n(R)=\frac{1}{R} \quad \text{(for } R\geq L_0\text{, the horizon).(9)}$$

This could also be obtained from conformal transformation optics [5, 41], with $n_z=n_w|\frac{dw}{dz}|$ for $n_w=1$ and $w=\ln z$ [42], where $R=|z|$ and $n_z=n(R)$. For any $R\geq L_0$, light will travel in circles, as it is mapped to the real coordinate of w. *In other words, such a profile will have infinite numbers of photon spheres.* However, for profile in Eq. (7), the unique photon sphere is at $R=(2+\sqrt{3})\frac{L}{4}$, which is mapped from $r=\frac{3L}{2}$ (See Appendix A). In Fig. 2(a), we put a point source at the photon sphere. We find that part of the rays will escape from the black hole, and part will be trapped by the photon sphere and approach to the horizon perpendicularly. In fact, for the rays emit to the left direction, which is under the photon sphere, they will all be trapped and incident on the event horizon perpendicularly. While for the rays emit to the right direction, which is outside the photon sphere, they will all be bent and escape the event horizon. We also plot the field pattern in wave optics for a point source in Fig. 2(b). The wave will interfere with each other at the opposite site of the source. The same trick was used here that we make the radius of horizon slightly larger in wave simulations than $\frac{L}{4}$ (here L is 1) to better present the field pattern and prevent wave approaching the singularity of the event horizon. The same way applied to Fig. 2(d).

It is because of the photon sphere that we could see the donut-liked halo from the earth [3]. We

therefore study the case of parallel light rays incident to the black hole in Fig. 2(c). For rays outside the photon sphere, they will be bent due to the gravitational lens effect of the black hole. For the rays incident almost tangential to the photon sphere, they will propagate in a U-turn trajectory, just like the Eaton lens [43, 44]. For the rays imping at the photon sphere, they will all be trapped and approach to the horizon perpendicularly. We also study the case for wave optics, i.e., an incident Gaussian beam interacts with the black hole. The field pattern is plot in Fig. 2(d), where we can see that the wave will be absorbed in the middle part, while for those outside the photon sphere, they could escape and will interfere with each other at the opposite site. For simplicity, the above simulations are performed in two dimensions. Obviously, our model could, at least in the optical system, commendably mimic the real effects of general relativity. It is because our equivalent isotropic refractive index profile is calculated directly from the metric formula of the corresponding space, such that the property of the analogue space can be well maintained.

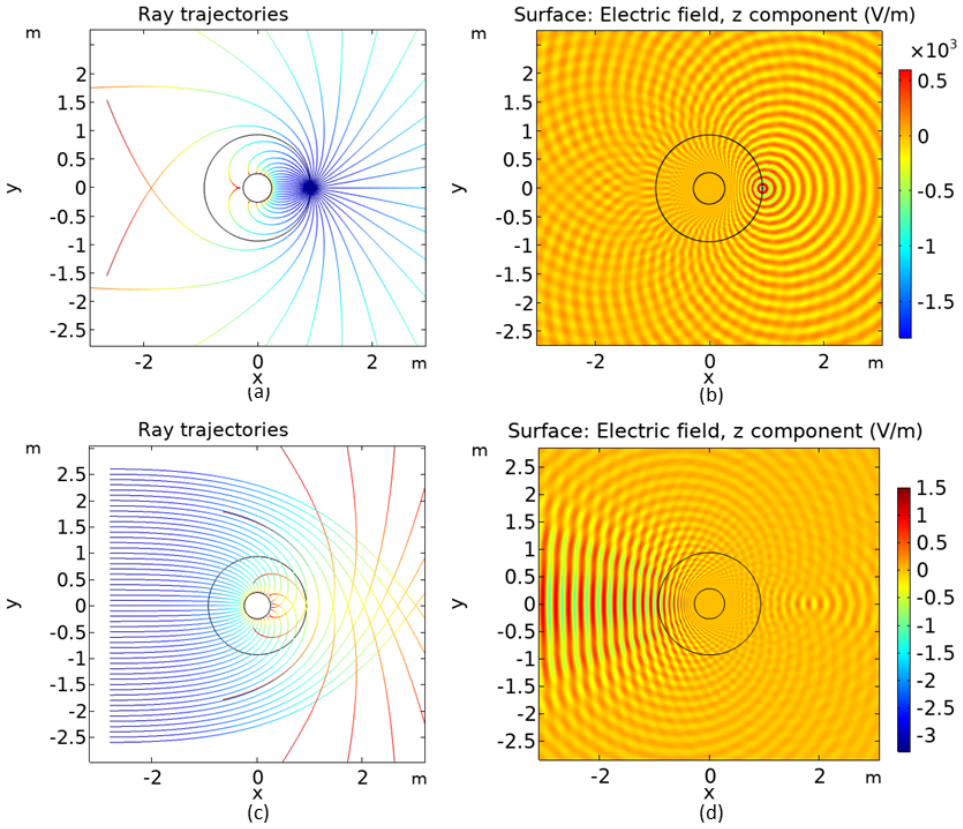

Fig. 2 A point source at the photon sphere of a black hole lens: (a) the ray trajectories; (b) the field pattern. (c) Parallel light rays incident to the black hole lens. (d) Gaussian beam incident to the black hole lens.

To visualize the appearance of the refractive-index profile given in Eq. (7), we have added to our scientific ray-tracer Dr TIM [33] the capability to trace rays in transformation-optics media. A 4th-order Runge-Kutta algorithm is used to solve the Hamilton-type equations, derived in Ref. [45], describing ray propagation in inhomogeneous transformation-optics media. Note that we can use a slightly modified refractive index profile with a same photon sphere to a Schwarzschild black hole (See Appendix B).

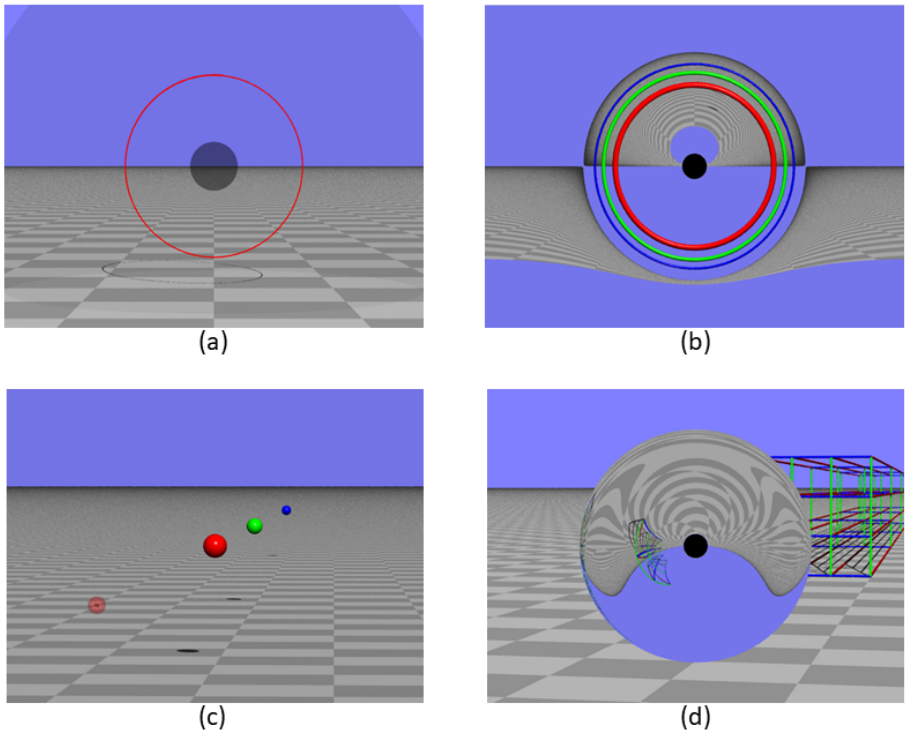

Fig. 3 Visualization using rendering raytracing of the appearance of the artificial black hole. (a) Two orbits of a ray trajectory (red line) on the photon sphere. The event horizon is indicated by a gray sphere in the center. (b) Small spheres placed behind the black hole appear as rings. The geometry of the setup is shown in (c), with the event horizon indicated as a small gray sphere inside a semitransparent red sphere that indicates the photon sphere. (d) Simulation of a scene containing a 3D lattice seen through a sphere of radius 1 filled with the refractive-index distribution. The horizon radius is 0.2 in (a) and 0.01 in (b-d). In (b), the refractive-index distribution was simulated in a sphere of radius 5 (n=1.008 on the edge).

After confirming that Dr. TIM correctly simulated a ray on the photon sphere (Fig. 3(a)), we simulated the appearance of objects, in our case small spheres, located behind the black hole (Fig. 3(c)). In complete analogy to the Einstein rings, these small spheres become distorted into rings (Fig. 3(b)). Finally, Fig. 3(d) shows the appearance of a scene containing a 3D lattice partially seen through a sphere filled with the refractive-index distribution. The image of the lattice and the space around it shows a strong rotation and distortion, which not only reveal the gravitational lensing effect but also leave us some hints on investigating the objects near the black hole. This gravitational lensing effect for an approximation of a refractive index profile in the infinity is also discussed in Appendix C.

III. Conclusion

In conclusion, based on general relativity in electrical engineering and transformation optics, we propose a series of radial spatial mappings to get the equivalent isotropic refractive index profiles

directly from the metric formulas of some static spaces in general relativity. We find that, the equivalent lens of de Sitter space is exactly Poincaré disk and also similar to a zero index lens, while that of Anti de Sitter space is simply Maxwell's fish-eye lens. In particular, we analyze a previous version of "optical black hole" and find that it has infinite photon spheres, while our black hole only has a unique photon sphere, which is the reason of the famous donut-liked halo of a realistic black hole. We study the light behavior and wave pattern in the de Sitter space and outside the black hole both from geometrical optics and wave optics. We could realize the black hole halo by 2D figures with the source of a point or some parallel light rays (Gaussian beam). Most importantly, with the isotropic refractive index profile in hand, we utilize our TIM program to visualize the black hole. The scenes not only indicate the ray trajectories outside the event horizon and that on the photon sphere, but also present the gravitational lensing effect and Einstein's rings around the event horizon. Moreover, we can see the image of a 3D lattice through the black hole lens intuitively as a view point of an observer opposite the lattice. These images could enhance our understanding of black hole and maybe we could find some new objects around the black hole according to the images. Hence, by further combining transformation optics and electrical general relativity, we could visualize a series of spaces, cosmic phenomena or some hypothetical concepts using TIM program for the future research, such as artificial wormholes [46, 47]. This effect can be considered as electromagnetic phenomena (lensing effect). In fact, we exactly mimic the famous spaces by using their equivalent materials in the framework of electromagnetism based on the transformation optics method. The similar effects of 4-dimension spacetimes are also worth studying in the future.

Acknowledgements

This work was supported by the National Science Foundation of China (Grant No. 11874311) and the Fundamental Research Funds for the Central Universities (Grant No. 20720170015). J.B. was supported by the UK's Engineering and Physical Sciences Research Council [grant number EP/N/509668/1]. R.X.M. was supported by the funding of Sun Yat-Sen University.

Appendix

A. The unique photon sphere of the refractive index profile Eq. (7).

Consider a light ray in a medium described by isotropic metric g_{ij} (expressed in spherical coordinates (r,θ,ϕ))

$$g_{ij} = n^2(r) \times \mathrm{diag}(1, r^2, r^2 \sin^2\theta). \tag{1}$$

Since the space described by such a metric is isotropic, the problem is effectively two-dimensional, which enables us to make a choice $\theta = \pi/2$. The light ray trajectory $\left(r(\lambda), \pi/2, \phi(\lambda)\right)$,

parameterized by λ, then satisfies the geodesic equations

$$\dot{\phi} = \frac{\mathrm{L}}{n^2(r)r^2} \tag{2}$$

$$\ddot{r} = \left[1 + \frac{r}{n(r)}\frac{\mathrm{d}\,n(r)}{\mathrm{d}r}\right]\frac{L^2}{n^4(r)r^3} - \dot{r}^2\frac{1}{n(r)}\frac{\mathrm{d}\,n(r)}{\mathrm{d}r}, \tag{3}$$

where $\dot{\phi} = \mathrm{d}\phi/\mathrm{d}\lambda$, $\dot{r} = \mathrm{d}r/\mathrm{d}\lambda$ and L is a constant. Light-ray trajectories in a medium with refractive-index profile $n(r)$ given by formula

$$n(r) = \frac{(r + R_{KB})^3}{r^2\left(r - R_{KB}\right)} \tag{4}$$

follow similar geodesic equations to those around a Schwarzschild black hole, i.e. a black hole described by Schwarzschild metric and $R_{KB} = \frac{L}{4}$ in the main text (Eq. 7). One of the features of a Schwarzschild black hole is the *photon sphere*, a location where the light rays can travel in circles. The radius q of a "photon sphere" in a medium $n(r)$ can be found as following: on the photon sphere, $\dot{r} = \ddot{r} = 0$. This is satisfied if and only if the square bracket in Eq. (3) equals zero for $r = q$, i.e.

$$1 + \frac{q}{n(q)}\frac{\mathrm{d}\,n}{\mathrm{d}r}\bigg|_{r\,=\,q} = 0. \tag{5}$$

If one inserts refractive-index profile $n(r)$, given by Eq. (4), to Eq. (5), the following equation is obtained

$$\frac{q^2 - 4qR_{KB} + R_{KB}^{\ 2}}{q^2 - R_{KB}^{\ 2}} = 0, \tag{6}$$

when solved for q

$$q = R_{KB}\left(2 + \sqrt{3}\right). \tag{7}$$

B. A modified refractive index profile to obtain a same photon sphere of a Schwarzschild black hole.

The radius of a photon sphere around a Schwarzschild black hole equals $3R/2$. This discrepancy can be fixed by inserting a parameter j to formula (4) as following

$$n_{KB}(r) = \frac{\left(r + jR\right)^3}{r^2\left(r - R\right)}. \tag{8}$$

For such a distribution, the radius q of a photon sphere equals

$$q = R\left(j+1+\sqrt{(j+1)^2 - j} \right). \tag{9}$$

To satisfy a requirement $q = 3R/2$, one can solve Eq. (9) for j, yielding a value $j = -3/8$.

C. Gravitational lensing effect for an approximation of refractive index profile in the infinity.

At distance r much larger than the Schwarzschild radius R_S, i.e. if $r \gg R_S$, the space-time around a Schwarzschild black hole can be approximated by a refractive-index distribution $n_S(r)$

$$n_S(r) = 1 + 2\frac{R_S}{r}. \tag{10}$$

If a light ray, travelling from infinity, passes around the black hole at distance b, it will be deflected by an angle $\Delta\theta(b)$

$$\Delta\theta(b) = 2\frac{R_S}{b}. \tag{11}$$

If a light source is placed exactly behind the lensing black hole at distance D_{SL} from that black hole, an observer at distance D_L will observe a ring around the black hole of an Einstein's radius, with a characteristic angle θ_E

$$\theta_E = \sqrt{2R_S \frac{D_{SL}}{(D_{SL} + D_L)D_L}}. \tag{12}$$

Very similar results can be obtained with our index profile given by Eq. (8). For $r \gg R$, the refractive-index profile can be approximated

$$n_{KB}(r) \approx 1 + 2\frac{\frac{3j+1}{2}R}{r}. \tag{13}$$

This implies that one can simply substitute $R_S \to (3j+1)R/2$ to the formulas well-known for weak gravitational lensing and will obtain the correct values.

References

[1] A. Einstein, Sitzungsber. K. Preuss. Akad. Wiss. 1, 688 (1916); A. Einstein, Sitzungsber. K. Preuss. Akad. Wiss. 1, 154 (1918).

[2] Abbott, B. P. et al. Observation of Gravitational Waves from a Binary Black Hole Merger, Phys. Rev. Lett. 116, 061102 (2016).

[3] The Event Horizon Telescope Collaboration et al. Astrophys. J. Lett. 875, L1-L5 (2019).

[4] U. Leonhardt and T. G. Philbin, General Relativity in Electrical Engineering, New J. Phys. 8, 247

(2006).
[5] U. Leonhardt, Optical conformal mapping, Science 312, 1777–1780 (2006).
[6] J. B. Pendry, D. Schurig, and D. R. Smith, Controlling electromagnetic fields, Science 312, 1780–1782 (2006).
[7] M. McCall, J. B. Pendry, V. Galdi, Y. Lai, S. A. R. Horsley, J. Li, J. Zhu, R. C. M. Thomas, O. Q. Teruel, P. Tassin, V. Ginis, E. Martini, G. Minatti, S. Maci, M. Ebrahimpouri, Y. Hao, P. Kinsler, J. Gratus, J. M. Lukens, A. M. Weiner, U. Leonhardt, I. I. Smolyaninov, V. N. Smolyaninova, R. T. Thompson, M. Wegener, M. Kadic and S. A. Cummer, Roadmap on transformation optics, J. Opt. 20, 063001 (2018).
[8] H. Chen and C. Chan, Transformation media that rotate electromagnetic fields, Appl. Phys. Lett. 90, 241105 (2007).
[9] H. Chen, B. Hou, S. Chen, X. Ao, W. Wen and C. Chan, Design and Experimental Realization of a Broadband Transformation Media Field Rotator at Microwave Frequencies, Phys. Rev. Lett. 102, 183903 (2009).
[10] M. Rahm, D. Schurig, D. A. Roberts, S. A. Cummer, D. R. Smith and J. B. Pendry, Design of electromagnetic cloaks and concentrators using form-invariant coordinate transformations of Maxwell's equations, Photonic. Nanostruct. 6, 87 (2008).
[11] C. Y. Li, L. Xu, L. L. Zhu, S. Y. Zou, Q. H. Liu, Z. Y. Wang and Huanyang Chen, Concentrators for Water Waves, Phys. Rev. Lett. 121, 104501 (2018).
[12] D. Shurig, J. B. Pendry and D. R. Smith, Opt. Express 15, 14772–82 (2007).
[13] U. Leonhardt and T. G. Philbin, Phys. Rev. A 81, 011804 (2010).
[14] V. Ginis, P. Tassin, J. Danckaert, C. M. Soukoulis and I. Veretennicoff, Creating electromagnetic cavities using transformation optics, New J. Phys. 14, 033007 (2012).
[15] H. Y. Chen, R.-X. Miao, and M. Li, Transformation optics that mimics the system outside a Schwarzschild black hole, Opt. Express 18, 15183-15188 (2010).
[16] S. S. Hegde and C. V. Vishveshwara, Optical analogues of spherically symmetric black hole spacetimes, J. Phys.: Conf. Ser. 484 012017 (2014).
[17] V. Ginis, P. Tassin, B. Craps and I. Veretennicoff, Frequency converter implementing an optical analogue of the cosmological redshift, Opt. Express 18, 5350-5355 (2010).
[18] M. Li, R.-X. Miao, and Y. Pang, Casimir energy, holographic dark energy and electromagnetic metamaterial mimicking de Sitter, Phys. Lett. B 689, 55–59 (2010).
[19] M. Li, R.-X. Miao, and Y. Pang, More studies on Metamaterials Mimicking de Sitter space, Opt. Express 18, 9026–9033 (2010).
[20] S.R. Boston, Time travel in transformation optics: Metamaterials with closed null geodesics, Physical Review D 91, 124035 (2015).
[21] T. G. Mackay and A. Lakhtakia, Towards a realization of Schwarzschild-(anti-)de Sitter spacetime as a particulate metamaterial, Phys. Rev. B 83, 195424 (2011)
[22] D. A. Genov, S. Zhang, and X. Zhang, Mimicking celestial mechanics in metamaterials, Nat. Phys. 5, 687–692 (2009).
[23] E. E. Narimanov and A. V. Kildishev, Optical black hole: Broadband omnidirectional light absorber, Appl. Phys. Lett. 95, 041106 (2009).
[24] C. Argyropoulos, E. Kallos, and Y. Hao, FDTD analysis of the optical black hole, JOSAB 27, 2020-2025 (2010).
[25] Q. Cheng, T. J. Cui, W. X. Jiang and B. G. Cai, An omnidirectional electromagnetic absorber made of metamaterials, New J. Phys. 12, 063006 (2010).

[26] C. Sheng, H. Liu, Y. Wang, S. N. Zhu and D. Genov, Trapping light by mimicking gravitational lensing, Nature Photonics 7, 902 (2013).
[27] C. Sheng, R. Bekenstein, H. Liu, S.N. Zhu and M. Segev, Wavefront shaping through emulated curved space in waveguide settings, Nature Communications 7, 10747 (2016).
[28] C. Sheng, H. Liu, H. Y. Chen and S. N. Zhu, Definite photon deflections of topological defects in metasurfaces and symmetry-breaking phase transitions with material loss, Nature Communications 9, 4271 (2018).
[29] V. Perlick, On Fermat's principle in general relativity: I. The general case, Classical and Quantum Gravity 7, 1319 (1990).
[30] V. Perlick, On Fermat's principle in general relativity: II. The conformally stationary case, Classical and Quantum Gravity 7, 1849 (1990).
[31] M. Šarbort and T. Tyc, Spherical media and geodesic lenses in geometrical optics, J. Opt. 14, 075705 (2012).
[32] L. Xu, X. Y. Wang, T. Tyc, C. Sheng, S. N. Zhu, H. Liu and H. Y. Chen, Light rays and waves on geodesic lenses, Photonics Res. 7, 1266-1272 (2019).
[33] S. Oxburgh, T. Tyc, and J. Courtial, Dr TIM: Ray-tracer TIM, with additional specialist scientific capabilities, Comp. Phys. Commun. 185, 1027–1037 (2014).
[34] A. Cvetkovski and M. Crovella, Multidimensional Scaling in the Poincare Disk, arXiv: 1105.5332v3 (2016).
[35] É. Ghys, Poincaré and his disk, The scientific legacy of Poincaré 36, 17-46.
[36] Q. Cheng, W. X. Jiang, and T. J. Cui, Spatial Power Combination for Omnidirectional Radiation via Anisotropic Metamaterials, Phys. Rev. Lett. 108, 213903 (2012).
[37] J. C. Maxwell, Solutions of problems, Camb. Dublin Math. J. 8, 188 (1854).
[38] S. Khorasani and B. Rashidian, Optical anisotropy of schwarzschild metric within equivalent medium framework, Opt. Comm. 283, 1222-1228 (2010).
[39] R. Doran, F.S.N. Lobo and P. Crawford, Interior of a Schwarzschild Black Hole Revisited, Found. Phys. 38, 160–187 (2008).
[40] H. Kawai and Y. Yokokura, Interior of black holes and information recovery, Phys. Rev. D 93, 044011 (2016).
[41] L. Xu and H. Y. Chen, Conformal Transformation Optics, Nature Photonics 9, 15-23 (2015).
[42] U. Leonhardt and T. Philbin, Geometry and Light: The Science of Invisibility (Courier Corporation, Chelmsford, MA, 2012).
[43] J. E. Eaton, On spherically symmetric lenses, Trans. IRE Antennas Propag. 4, 66 (1952).
[44] A. J. Danner, and U. Leonhardt, Lossless design of an Eaton lens and invisible sphere by transformation optics with no bandwidth limitation, International Quantum Electronics Conference. Optical Society of America, (2009).
[45] D. Schurig, J. B. Pendry, and D. R. Smith, Calculation of material properties and ray tracing in transformation media, Opt. Express 14, 9794-9804 (2006)
[46] A. Greenleaf, M. Lassas, and G. Uhlmann, Electromagnetic wormholes and virtual magnetic monopoles from metamaterials, Phys. Rev. Lett. 99, 183901 (2007).
[47] J. Zhu, Y. Liu, Z. Liang, T. Chen, and J. Li, Elastic waves in curved space: mimicking a wormhole, Physical Review Letters 121, 234301 (2018).